

Research Article

Nonlinear Vibrations of Multiwalled Carbon Nanotubes under Various Boundary Conditions

Hossein Aminikhah¹ and Milad Hemmatnezhad²

¹ Department of Applied Mathematics, School of Mathematical Sciences, University of Guilan, P.O. Box 1914, Rasht 41938, Iran

² Faculty of Mechanical Engineering, Takestan Branch, Islamic Azad University, P.O. Box 3351, Takestan 58937, Iran

Correspondence should be addressed to Hossein Aminikhah, hossein.aminikhah@gmail.com

Received 7 May 2011; Accepted 20 June 2011

Academic Editor: S. Grace

Copyright © 2011 H. Aminikhah and M. Hemmatnezhad. This is an open access article distributed under the Creative Commons Attribution License, which permits unrestricted use, distribution, and reproduction in any medium, provided the original work is properly cited.

The present work deals with applying the homotopy perturbation method to the problem of the nonlinear oscillations of multiwalled carbon nanotubes embedded in an elastic medium under various boundary conditions. A multiple-beam model is utilized in which the governing equations of each layer are coupled with those of its adjacent ones via the van der Waals interlayer forces. The amplitude-frequency curves for large-amplitude vibrations of single-walled, double-walled, and triple-walled carbon nanotubes are obtained. The influences of some commonly used boundary conditions, changes in material constant of the surrounding elastic medium, and variations of the nanotubes geometrical parameters on the vibration characteristics of multiwalled carbon nanotubes are discussed. The comparison of the generated results with those from the open literature illustrates that the solutions obtained are of very high accuracy and clarifies the capability and the simplicity of the present method. It is worthwhile to say that the results generated are new and can be served as a benchmark for future works.

1. Introduction

In recent years, considerable effort has been devoted to the subject area of nanotechnology. Since nanomaterials possess unique mechanical, physical, and chemical properties, they occupy the chief topic of research in many scientific fields. Nowadays, they are being used as the substantial parts of nanoelectronics, nanodevices, and nanocomposites. Amongst the materials at the scale of nanometers, carbon nanotubes (CNTs) discovered by Iijima [1] in 1991 have attracted intense interest to many research workers. In spite of being too small and having light weight, CNTs have a very large Young's modulus up to 1 TPa in the axial direction. A good review on their properties and industrial applications can be found detailed in [2]. The application of analytical and numerical approaches to the

study of CNTs is suggested recently [3–5]. Since the vibrations of CNTs are of considerable importance in a number of nanomechanical devices such as oscillators, charge detectors, field emission devices, and sensors, many researches have been so far devoted to the problem of the vibration of these nanomaterials [6–11]. However, most of the investigations conducted on the vibration of CNTs have been restricted to the linear regime. Fu et al. [12] studied the nonlinear vibrations of embedded nanotubes using the incremental harmonic balanced method (IHBM). In that work, single-walled nanotubes (SWNTs) and double-walled nanotubes (DWNNTs) with simply supported end conditions were considered for the study. Recently, He [5] applied the homotopy perturbation method (HPM) to investigate the nonlinear vibrations of MWNTs using the same beam model as the one used in [12]. In that paper, they also extended Fu's work to the problem of triple-walled nanotubes (TWNNTs) and gave the nonlinear amplitude-frequency curves. The present work is an extension of the authors' previous work for free nonlinear oscillations of MWNTs with arbitrary boundary conditions. The HPM as a powerful analytical approach was first introduced by He [13–20] and has been used by many mathematicians and engineers to solve various functional equations. In this method, the solution is considered as the summation of an infinite series which converges rapidly to the exact solution. Some applications of this method are summarized in a review article by He [21]. This simple method has been applied to solve linear and nonlinear equations of heat transfer [22–24], fluid mechanics [25], nonlinear Schrödinger equations [26], nonlinear oscillations [27, 28], some boundary value problems, and other subjects in different disciplines [29]. The recent developments of this perturbation-based method can be found in [30]. The convergence study of HPM for partial differential equations has been recently reported in [31]. The aim of this investigation is to show the effectiveness of HPM and the capability of this simple method for handling the nonlinear oscillations of many vibrating systems. It is shown that the first approximate solution of New HPM admits a remarkable accuracy in comparison with the results obtained from the incremental harmonic balanced method for the amplitude-frequency curves.

2. Basic Equations

Consider a CNT of length L , Young's modulus E , density ρ , cross-sectional area A , and cross-sectional inertia moment I , embedded in an elastic medium with constant k determined by the material constants of the surrounding medium. This model is shown in Figure 1. Assume that u and w are the displacements of the nanotube along x and z directions respectively in terms of the spatial coordinate x and the time variable t .

The free vibration governing equation of this embedded beam-modeled CNT considering the geometric nonlinearity is [12]

$$\rho A \frac{\partial^2 w}{\partial t^2} + EI \frac{\partial^4 w}{\partial x^4} = \left[\frac{EA}{2L} \int_0^L \left(\left(\frac{\partial v}{\partial x} \right)^2 + \left(\frac{\partial w}{\partial x} \right)^2 \right) dx \right] \frac{\partial^2 w}{\partial x^2} + P, \quad (2.1)$$

where P is the transverse load considered as the interaction pressure per unit axial length between the outermost tube and the surrounding medium, which can be described by the Winkler model [32, 33] as

$$P(x, t) = -kw. \quad (2.2)$$

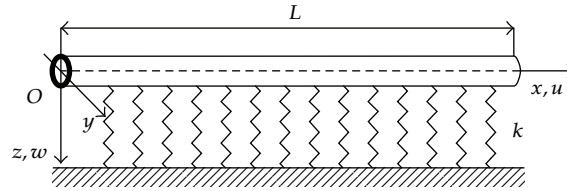


Figure 1: Model of an embedded carbon nanotube.

Herein, the negative sign indicates that the pressure P is opposite to the deflection of the outermost tube. Substituting (2.2) into (2.1) we get

$$\rho A \frac{\partial^2 w}{\partial t^2} + EI \frac{\partial^4 w}{\partial x^4} + kw = \left[\frac{EA}{2L} \int_0^L \left(\frac{\partial w}{\partial x} \right)^2 dx \right] \frac{\partial^2 w}{\partial x^2}. \quad (2.3)$$

For a MWNT with N layers, the pressure at any point between any two adjacent tubes, denoted as the van der Waals forces, can be expressed as

$$F_i = c_i(w_i - w_{i-1}), \quad (2.4)$$

where F_i is the van der Waals force between the i th tube and the $i-1$ th tube. c_i is the coefficient of the van der Waals force between the i th tube and the $i-1$ th tube defined according to [34]. Therefore, imposing the effects of the van der Waals forces to (2.3) it results in the n coupled nonlinear differential equations corresponding to the transverse nonlinear vibrations of an embedded MWNT with n layers

$$\begin{aligned} EI_1 \frac{\partial^4 w_1}{\partial x^4} + \rho A_1 \frac{\partial^2 w_1}{\partial t^2} &= \left[\frac{EA_1}{2l} \int_0^L \left(\frac{\partial w_1}{\partial x} \right)^2 dx \right] \frac{\partial^2 w_1}{\partial x^2} + c_1(w_2 - w_1), \\ EI_2 \frac{\partial^4 w_2}{\partial x^4} + \rho A_2 \frac{\partial^2 w_2}{\partial t^2} &= \left[\frac{EA_2}{2l} \int_0^L \left(\frac{\partial w_2}{\partial x} \right)^2 dx \right] \frac{\partial^2 w_2}{\partial x^2} + c_2(w_3 - w_2) - c_1(w_2 - w_1), \\ &\vdots \\ EI_n \frac{\partial^4 w_n}{\partial x^4} + \rho A_n \frac{\partial^2 w_n}{\partial t^2} &= \left[\frac{EA_n}{2l} \int_0^L \left(\frac{\partial w_n}{\partial x} \right)^2 dx \right] \frac{\partial^2 w_n}{\partial x^2} - kw_n - c_{n-1}(w_n - w_{n-1}). \end{aligned} \quad (2.5)$$

Assuming $w_i(x, t) = \varphi(x)W_i(t)$, $i = 1, 2, \dots, n$, where $\varphi(x)$ is the first eigenmode of the beam satisfying the kinematic boundary conditions [34] and $W_i(t)$ is the time-dependent

deflection parameter of the i th layer of the nanotube and applying the Galerkin method, the governing equations of motion are obtained as follows:

$$\begin{aligned}
 EI_1 W_1 \alpha_1 + \left(\rho A_1 \frac{d^2 W_1}{dt^2} + c_1 W_1 - c_1 W_2 \right) \alpha_2 - \frac{EA_1}{2l} W_1^3 \alpha_3 &= 0, \\
 EI_2 W_2 \alpha_1 + \left(\rho A_2 \frac{d^2 W_2}{dt^2} + c_1 W_2 - c_1 W_1 + c_2 W_2 - c_2 W_3 \right) \alpha_2 - \frac{EA_2}{2l} W_2^3 \alpha_3 &= 0, \\
 &\vdots \\
 EI_n W_n \alpha_1 + \left(\rho A_n \frac{\partial^2 W_n}{\partial t^2} + c_{n-1} (W_n - W_{n-1}) + k W_n \right) - \frac{EA_n}{2l} W_n^3 \alpha_3 &= 0.
 \end{aligned} \tag{2.6}$$

The above equations are the differential equations of motion governing the nonlinear vibrations of CNTs subjected to the following initial conditions:

$$W_i(0) = W_{\max}, \quad \frac{dW_i(0)}{dt} = 0, \quad (i = 1, 2, \dots, n), \tag{2.7}$$

where W_{\max} denotes the maximum amplitude of oscillation. In (2.6), α_1 , α_2 , and α_3 are as follows:

$$\begin{aligned}
 \alpha_1 &= \int_0^L \left(\frac{d^4 \varphi(x)}{dx^4} \right) \varphi(x) dx, \\
 \alpha_2 &= \int_0^L \varphi^2(x) dx, \\
 \alpha_3 &= \int_0^L \left[\frac{d^2 \varphi(x)}{dx^2} \int_0^L \left(\frac{d\varphi(x)}{dx} \right)^2 dx \right] \varphi(x) dx.
 \end{aligned} \tag{2.8}$$

The deflection of the nanotube is subjected to the following boundary conditions.

For a simply supported (S-S) nanotube,

$$w(0, t) = 0, \quad \frac{\partial^2 w(0, t)}{\partial x^2} = 0, \quad w(L, t) = 0, \quad \frac{\partial^2 w(L, t)}{\partial x^2} = 0. \tag{2.9}$$

For a clamped-clamped (C-C) nanotube,

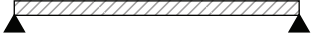
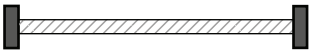

$$w(0, t) = 0, \quad \frac{\partial w(0, t)}{\partial x} = 0, \quad w(L, t) = 0, \quad \frac{\partial w(L, t)}{\partial x} = 0. \tag{2.10}$$

For a clamped-simply supported (C-S) nanotube,

$$w(0, t) = 0, \quad \frac{\partial w(0, t)}{\partial x} = 0, \quad w(L, t) = 0, \quad \frac{\partial^2 w(L, t)}{\partial x^2} = 0. \tag{2.11}$$

The base functions corresponding to the above boundary conditions are given in Table 1.

Table 1: Common boundary conditions for the transverse vibration of beams.

End conditions of beam	Mode shape (normal function)	Value of β
Simply supported 	$\sin\left(\frac{\beta x}{L}\right)$	π
Clamped-Clamped 	$\left(\cosh\left(\frac{\beta x}{L}\right) - \cos\left(\frac{\beta x}{L}\right)\right)$ $-\left(\frac{\cosh \beta - \cos \beta}{\sinh \beta - \sin \beta}\right)\left(\sinh\left(\frac{\beta x}{L}\right) - \sin\left(\frac{\beta x}{L}\right)\right)$	4.730041
Clamped-Simply supported 	$\left(\cosh\left(\frac{\beta x}{L}\right) - \cos\left(\frac{\beta x}{L}\right)\right)$ $-\left(\frac{\cosh \beta - \cos \beta}{\sinh \beta - \sin \beta}\right)\left(\sinh\left(\frac{\beta x}{L}\right) - \sin\left(\frac{\beta x}{L}\right)\right)$	3.926602

3. Application of HPM

3.1. Applying a New HPM for Nonlinear Vibrations of an SWNT

For an SWNT, the nonlinear vibration governing equation is given by (2.6) with $n = 1$ as follows:

$$\frac{d^2 W}{dt^2} + \left(\frac{EI}{\rho A} \frac{\alpha_1}{\alpha_2} + \frac{k}{\rho A} \right) W - \frac{E}{2\rho L} \frac{\alpha_3}{\alpha_2} W^3 = 0. \quad (3.1)$$

Under the transformations $r = \sqrt{I/A}$, $\tau = \omega t$, and $a = W/r$, the above equation can be transformed to the following nonlinear equation:

$$\omega^2 \frac{d^2 a}{d\tau^2} + f_1 a - f_2 a^3 = 0, \quad (3.2)$$

with f_1 and f_2 defined as

$$f_1 = \frac{EI}{\rho A} \frac{\alpha_1}{\alpha_2} + \frac{k}{\rho A} = \omega_b^2, \quad f_2 = \frac{EI}{2\rho AL} \frac{\alpha_3}{\alpha_2}. \quad (3.3)$$

In (3.2), $\sqrt{f_1} = \omega_b$ is the linear, free vibration frequency, and ω is an unknown angular frequency to be determined. Now, we apply a New HPM to seek the solution of (3.1). To this aim, we construct the following homotopy with ω_0 as the initial approximation for the angular frequency:

$$(1-p)\omega_0^2 \left(\frac{d^2 a}{d\tau^2} + a \right) + p \left(\omega^2 \frac{d^2 a}{d\tau^2} + f_1 a - f_2 a^3 \right) = 0. \quad (3.4)$$

Here p is an embedding parameter, $a = a(\tau, p)$, and $\omega = \omega(p)$. Clearly, when $p = 0$, (3.4) yields the linear harmonic

$$\frac{d^2 a}{d\tau^2} + a = 0, \quad a(0) = X, \quad \frac{da(0)}{d\tau} = 0, \quad (3.5)$$

and, for $p = 1$, it results the nonlinear equation (3.1). As embedding parameter p travels from 0 to 1, the solutions $a = a(\tau, p)$ and $\omega = \omega(p)$ of the homotopy (3.4) change from their initial approximations $a_0(\tau)$ and ω_0 to the required solutions $a(\tau)$ and ω of (3.1).

Suppose the solution of (3.2) to be in the following form:

$$\begin{aligned} a(\tau) &= a_0(\tau) + p a_1(\tau) + p^2 a_2(\tau) + \cdots, \\ \omega &= \omega_0 + p \omega_1 + p^2 \omega_2 + \cdots. \end{aligned} \quad (3.6)$$

Substituting the above relations into the homotopy equation (3.4) and rearranging the coefficients of the terms with identical powers of p , we have a series of linear differential equations

$$\begin{aligned} p^0 : \frac{d^2 a_0}{d\tau^2} + a_0 &= 0, \quad a_0(0) = X, \quad \frac{da_0(0)}{d\tau} = 0, \\ p^1 : \omega_0^2 \left(\frac{d^2 a_1}{d\tau^2} + a_1 \right) - \omega_0^2 a_0 + f_1 a_0 - f_2 a_0^3 &= 0, \quad a_1(0) = 0, \quad \frac{da_1(0)}{d\tau} = 0, \\ p^2 : \omega_0^2 \left(\frac{d^2 a_2}{d\tau^2} + a_2 \right) - \omega_0^2 a_1 + 2\omega_0 \omega_1 \frac{d^2 a_0}{d\tau^2} + f_1 a_1 - 3f_2 a_0^2 a_1 &= 0, \\ a_2(0) &= 0, \quad \frac{da_2(0)}{d\tau} = 0, \\ &\vdots \end{aligned} \quad (3.7)$$

The solution of the initial zeroth approximation is simply given by

$$a_0(\tau) = X \cos \tau, \quad (3.8)$$

putting this into the first approximation equation, we get

$$\omega_0^2 \frac{d^2 a_1}{d\tau^2} + \omega_0^2 a_1 - \omega_0^2 X \cos \tau + f_1 X \cos \tau - f_2 X^3 \cos^3 \tau = 0. \quad (3.9)$$

Expanding the trigonometric function $\cos^3 \tau$ as $\cos^3 \tau = (3/4) \cos \tau + (1/4) \cos 3\tau$, and letting the coefficient of $\cos \tau$ to be zero in order to eliminate the secular terms, we arrive at

$$\omega_0 = \sqrt{f_1 - \frac{3}{4}f_2 X^2}. \quad (3.10)$$

Therefore, the ratio of the nonlinear frequency, ω_0 , to the linear frequency, ω_b , becomes

$$\Psi = \sqrt{1 - \frac{3}{4}\left(\frac{f_2}{f_1}\right)X^2}. \quad (3.11)$$

The solution of (3.9) can be easily achieved as

$$a_1(\tau) = \frac{f_2 X^3}{32f_1 - 24f_2 X^2} (\cos \tau - \cos 3\tau). \quad (3.12)$$

Thus, the first approximate solution of (3.2) can be written as follows:

$$a(\tau) = a_0(\tau) + a_1(\tau) = X \cos \tau + \frac{f_2 X^3}{32f_1 - 24f_2 X^2} (\cos \tau - \cos 3\tau). \quad (3.13)$$

3.2. Applying a New HPM for Nonlinear Vibrations of a DWNT

For a DWNT, the nonlinear vibration governing equation is given by (2.6) with $n = 2$ as follows:

$$\begin{aligned} \frac{d^2 W_1}{dt^2} + \left(\frac{EI_1}{\rho A_1} \frac{\alpha_1}{\alpha_2} + \frac{c_1}{\rho A_1} \right) W_1 - \frac{E}{2\rho L} \frac{\alpha_3}{\alpha_2} W_1^3 - \frac{c_1}{\rho A_1} W_2 &= 0, \\ \frac{d^2 W_2}{dt^2} + \left(\frac{EI_2}{\rho A_2} \frac{\alpha_1}{\alpha_2} + \frac{k}{\rho A_2} + \frac{c_1}{\rho A_2} \right) W_2 - \frac{E}{2\rho L} \frac{\alpha_3}{\alpha_2} W_2^3 - \frac{c_1}{\rho A_2} W_1 &= 0. \end{aligned} \quad (3.14)$$

Substituting the following dimensionless parameters

$$r = \sqrt{\frac{I_1}{A_1}}, \quad a_1 = \frac{W_1}{r}, \quad a_2 = \frac{W_2}{r}, \quad \tau = \omega t. \quad (3.15)$$

Equation (3.14) can be transformed to the following dimensionless nonlinear system of equations:

$$\begin{aligned}\omega^2 \frac{d^2 a_1}{dt^2} + f'_1 a_1 - f'_2 a_1^3 - f'_3 a_2 &= 0, \\ \omega^2 \frac{d^2 a_2}{dt^2} + f'_4 a_2 - f'_5 a_2^3 - f'_6 a_1 &= 0,\end{aligned}\tag{3.16}$$

with f'_1 to f'_6 defined as

$$\begin{aligned}f'_1 &= \left(\frac{EI_1}{\rho A_1} \frac{\alpha_1}{\alpha_2} + \frac{c_1}{\rho A_1} \right), & f'_1 &= \frac{EI_1}{2\rho A_1 L} \frac{\alpha_3}{\alpha_2}, & f'_3 &= \frac{c_1}{\rho A_1}, \\ f'_4 &= \left(\frac{EI_2}{\rho A_2} \frac{\alpha_1}{\alpha_2} + \frac{k}{\rho A_2} + \frac{c_1}{\rho A_2} \right), & f'_5 &= \frac{EI_1}{2\rho A_1 L} \frac{\alpha_3}{\alpha_2}, & f'_6 &= \frac{c_1}{\rho A_2}.\end{aligned}\tag{3.17}$$

In a similar manner as above, one constructs a homotopy on (3.16) as follows:

$$\begin{aligned}(1-p)\omega_0^2 \left(\frac{d^2 a_1}{d\tau^2} + a_1 \right) + p \left(\omega^2 \frac{d^2 a_1}{dt^2} + f'_1 a_1 - f'_2 a_1^3 - f'_3 a_2 \right) &= 0, \\ (1-p)\omega_0^2 \left(\frac{d^2 a_2}{d\tau^2} + a_2 \right) + p \left(\omega^2 \frac{d^2 a_2}{dt^2} + f'_4 a_2 - f'_5 a_2^3 - f'_6 a_1 \right) &= 0.\end{aligned}\tag{3.18}$$

Here, the solutions $a_1 = a_1(\tau, p)$, $a_2 = a_2(\tau, p)$, and $\omega = \omega(p)$ of the homotopy (3.18) change from their initial approximations $a_{10}(\tau)$, $a_{20}(\tau)$ and ω_0 to the required solutions $a_1(\tau)$, $a_2(\tau)$ and ω of (3.16) as the embedding parameter p travels from 0 to 1.

Suppose the solution of (3.18) to be in the following form

$$\begin{aligned}a_1(\tau) &= a_{10}(\tau) + p a_{11}(\tau) + p^2 a_{12}(\tau) + \cdots, \\ a_2(\tau) &= a_{20}(\tau) + p a_{21}(\tau) + p^2 a_{22}(\tau) + \cdots, \\ \omega &= \omega_0 + p \omega_1 + p^2 \omega_2 + \cdots.\end{aligned}\tag{3.19}$$

Substituting the above relations into the homotopy equation (3.18) and rearranging the coefficients of the terms with identical powers of p , we have a series of linear differential equations

$$\begin{aligned}
 p^0 : & \begin{cases} \frac{d^2 a_{10}}{d\tau^2} + a_{10} = 0, & a_{10}(0) = X_1, \quad \frac{da_{10}(0)}{d\tau} = 0, \\ \frac{d^2 a_{20}}{d\tau^2} + a_{20} = 0, & a_{20}(0) = X_2, \quad \frac{da_{20}(0)}{d\tau} = 0, \end{cases} \\
 p^1 : & \begin{cases} \omega_0^2 \left(\frac{d^2 a_{11}}{d\tau^2} + a_{11} \right) - \omega_0^2 a_{10} + f'_1 a_{10} - f'_2 a_{10}^3 - f'_3 a_{20} = 0, & a_{11}(0) = 0, \quad \frac{da_{11}(0)}{d\tau} = 0, \\ \omega_0^2 \left(\frac{d^2 a_{21}}{d\tau^2} + a_{21} \right) - \omega_0^2 a_{20} + f'_4 a_{20} - f'_5 a_{20}^3 - f'_6 a_{10} = 0, & a_{21}(0) = 0, \quad \frac{da_{21}(0)}{d\tau} = 0, \end{cases} \\
 & \vdots
 \end{aligned} \tag{3.20}$$

The solution of the initial zeroth approximation is simply given by

$$\begin{aligned}
 a_{10}(\tau) &= X_1 \cos \tau, \\
 a_{20}(\tau) &= X_2 \cos \tau.
 \end{aligned} \tag{3.21}$$

Substituting these into the first approximation together with eliminating the coefficient of $\cos \tau$ in the above system to avoid the secular terms it results in the following nonlinear system which can be easily solved using a simple mathematical algorithm such as Newton-Raphson technique:

$$\begin{aligned}
 -X_1 \omega_0^2 + f'_1 X_1 - \frac{3}{4} f'_2 X_1^3 - f'_3 X_2 &= 0, \\
 -X_2 \omega_0^2 + f'_4 X_2 - \frac{3}{4} f'_5 X_2^3 - f'_6 X_1 &= 0.
 \end{aligned} \tag{3.22}$$

3.3. Applying a New HPM for Nonlinear Vibrations of a TWNT

For a TWNT, the nonlinear vibration governing equation is given by (2.6) with $n = 3$ as follows:

$$\begin{aligned}
 \frac{d^2 W_1}{dt^2} + \left(\frac{EI_1}{\rho A_1} \frac{\alpha_1}{\alpha_2} + \frac{c_1}{\rho A_1} \right) W_1 - \frac{E}{2\rho L} \frac{\alpha_3}{\alpha_2} W_1^3 - \frac{c_1}{\rho A_1} W_2 &= 0, \\
 \frac{d^2 W_2}{dt^2} + \left(\frac{EI_2}{\rho A_2} \frac{\alpha_1}{\alpha_2} + \frac{c_1}{\rho A_2} + \frac{c_2}{\rho A_2} \right) W_2 - \frac{E}{2\rho L} \frac{\alpha_3}{\alpha_2} W_2^3 - \frac{c_1}{\rho A_2} W_1 - \frac{c_2}{\rho A_2} W_2 &= 0, \\
 \frac{d^2 W_3}{dt^2} + \left(\frac{EI_3}{\rho A_3} \frac{\alpha_1}{\alpha_2} + \frac{c_2}{\rho A_3} + \frac{k}{\rho A_3} \right) W_3 - \frac{E}{2\rho L} \frac{\alpha_3}{\alpha_2} W_3^3 - \frac{c_2}{\rho A_3} W_2 &= 0.
 \end{aligned} \tag{3.23}$$

Substituting the following dimensionless parameters:

$$r = \sqrt{\frac{I_1}{A_1}}, \quad a_1 = \frac{W_1}{r}, \quad a_2 = \frac{W_2}{r}, \quad a_3 = \frac{W_3}{r}, \quad \tau = \omega t. \quad (3.24)$$

Equation (3.3) can be transformed to the following dimensionless nonlinear system of equations:

$$\begin{aligned} \omega^2 \frac{d^2 a_1}{dt^2} + f_1'' a_1 - f_2'' a_1^3 - f_3'' a_2 &= 0, \\ \omega^2 \frac{d^2 a_2}{dt^2} + f_4'' a_2 - f_5'' a_2^3 - f_6'' a_1 - f_7'' a_3 &= 0, \\ \omega^2 \frac{d^2 a_3}{dt^2} + f_8'' a_3 - f_9'' a_3^3 - f_{10}'' a_2 &= 0, \end{aligned} \quad (3.25)$$

with f_1'' to f_{10}'' defined as

$$\begin{aligned} f_1'' &= \left(\frac{EI_1}{\rho A_1} \frac{\alpha_1}{\alpha_2} + \frac{c_1}{\rho A_1} \right), & f_2'' &= \frac{EI_1}{2\rho A_1 L} \frac{\alpha_3}{\alpha_2}, & f_3'' &= \frac{c_1}{\rho A_1}, \\ f_4'' &= \left(\frac{EI_2}{\rho A_2} \frac{\alpha_1}{\alpha_2} + \frac{c_1}{\rho A_2} + \frac{c_2}{\rho A_2} \right), & f_5'' &= \frac{EI_1}{2\rho A_1 L} \frac{\alpha_3}{\alpha_2}, & f_6'' &= \frac{c_1}{\rho A_2}, & f_7'' &= \frac{c_2}{\rho A_2}, \\ f_8'' &= \left(\frac{EI_3}{\rho A_3} \frac{\alpha_1}{\alpha_2} + \frac{c_2}{\rho A_3} + \frac{k}{\rho A_3} \right), & f_9'' &= \frac{EI_1}{2\rho A_1 L} \frac{\alpha_3}{\alpha_2}, & f_{10}'' &= \frac{c_2}{\rho A_3}. \end{aligned} \quad (3.26)$$

Likewise, we construct a homotopy on (3.25) as follows:

$$\begin{aligned} (1-p)\omega_0^2 \left(\frac{d^2 a_1}{d\tau^2} + a_1 \right) + p \left(\omega^2 \frac{d^2 a_1}{dt^2} + f_1'' a_1 - f_2'' a_1^3 - f_3'' a_2 \right) &= 0, \\ (1-p)\omega_0^2 \left(\frac{d^2 a_2}{d\tau^2} + a_2 \right) + p \left(\omega^2 \frac{d^2 a_2}{dt^2} + f_4'' a_2 - f_5'' a_2^3 - f_6'' a_1 - f_7'' a_3 \right) &= 0, \\ (1-p)\omega_0^2 \left(\frac{d^2 a_3}{d\tau^2} + a_3 \right) + p \left(\omega^2 \frac{d^2 a_3}{dt^2} + f_8'' a_3 - f_9'' a_3^3 - f_{10}'' a_2 \right) &= 0. \end{aligned} \quad (3.27)$$

Suppose the solution of (3.27) to be in the following form:

$$\begin{aligned}a_1(\tau) &= a_{10}(\tau) + p a_{11}(\tau) + p^2 a_{12}(\tau) + \cdots, \\a_2(\tau) &= a_{20}(\tau) + p a_{21}(\tau) + p^2 a_{22}(\tau) + \cdots, \\a_3(\tau) &= a_{30}(\tau) + p a_{31}(\tau) + p^2 a_{32}(\tau) + \cdots, \\ \omega &= \omega_0 + p \omega_1 + p^2 \omega_2 + \cdots.\end{aligned}\tag{3.28}$$

Taking $a_{10} = X_1 \cos \tau$, $a_{20} = X_2 \cos \tau$, and $a_{30} = X_3 \cos \tau$, as the initial guesses for a_1 , a_2 , and a_3 then eliminating secular terms as above, the first approximate solution appears in the following nonlinear system:

$$\begin{aligned}-X_1 \omega_0^2 + f_1'' X_1 - \frac{3}{4} f_2'' X_1^3 - f_3'' X_2 &= 0, \\-X_2 \omega_0^2 + f_4'' X_2 - \frac{3}{4} f_5'' X_2^3 - f_6'' X_1 - f_7'' X_3 &= 0, \\-X_3 \omega_0^2 + f_8'' X_3 - \frac{3}{4} f_9'' X_2^3 - f_{10}'' X_2 &= 0.\end{aligned}\tag{3.29}$$

Using the former solving process, the nonlinear amplitude frequency response curves can be obtained for TWNTs.

4. Discussion of Results

The material and geometric parameters of a CNT are taken as $E = 1.1$ TPa, $\rho = 1300$ kg/m³, $l = 45$ nm, the outer diameter $d_1 = 3$ nm, and the thickness of the each layer 0.68 nm. The amplitude-frequency response curves for a TWNT for several spring constants k are shown in Figure 2 in which Ψ is the ratio of the fundamental nonlinear frequency, ω to the fundamental linear frequency ω_b , and X is the maximum vibration amplitude. The fundamental linear frequency can be simply calculated by setting $W_i = W_{\max_i} \cos \omega_b t$, $i = 1, 2, \dots, n$, into nonlinear vibration governing equations of MWNTs without considering its nonlinear terms. Then, by setting the determinant of the achieved matrix equal to zero, the frequency characteristic equation will be obtained. The fundamental linear vibration frequency of MWNT is the lowest root of the resulting characteristic equation as illustrated in [35]. As can be seen from Figure 2, in contrast to linear systems, the nonlinear frequency is a function of amplitude so that the larger the amplitude, the more pronounced the discrepancy between the linear and nonlinear frequencies becomes. It is also seen that as the spring constant k increases, the nonlinear frequencies tend to approach the linear ones especially when k exceeds the value $k = 10^7$ N/m². It should be noted that the results are in an excellent agreement with those obtained via incremental harmonic balance method (IHBM) according to the formulations presented in [12]. Figure 3 shows the nonlinear to linear frequency ratio versus nondimensional amplitude ratio for three different boundary conditions and $k = 10^7$ N/m². Similar figures for DWNT and TWNT are illustrated in Figures 4 and 5. In Figures 4 and 5, the values of the coefficients of the van der Waals forces are $c_1 = c_2 = 0.3 \times 10^{12}$ N/m² and $k = 10^7$ N/m².

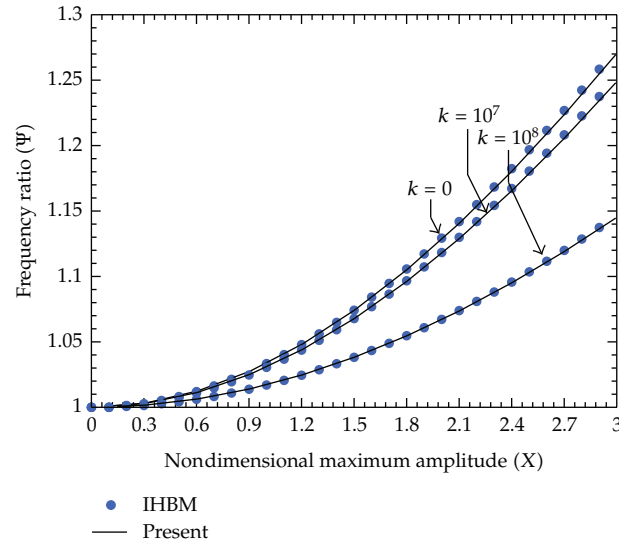


Figure 2: Effect of spring constant k on nonlinear amplitude frequency response curves of TWNT.

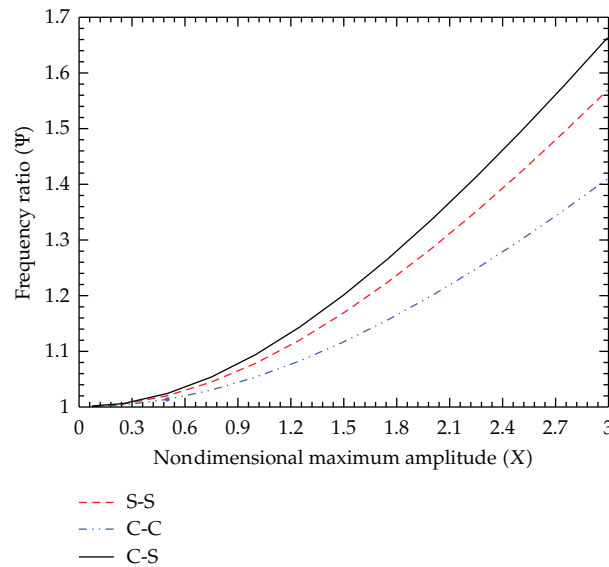


Figure 3: Nondimensional frequency ratio against nondimensional maximum amplitude of SWNTs under various boundary conditions ($k = 10^7 \text{ N/m}^2$).

Figure 6 illustrates the nonlinear frequency variation against length to radius ratio of a TWNT shell under different boundary conditions for $k = 10^7 \text{ N/m}^2$ and $X = 2$. It can be observed that with the increase of the aspect ratio of the nanotubes, the nonlinear vibration frequencies of MWNTs decrease. As is expected, the double clamped CNT has the highest natural frequency among the selected boundary conditions. A comparison between the nondimensional amplitude ratio of the first layer of a C-C SWNT and its linear counterpart is shown in Figure 7 for $k = 10^7 \text{ N/m}^2$. To demonstrate the accuracy of the obtained analytical

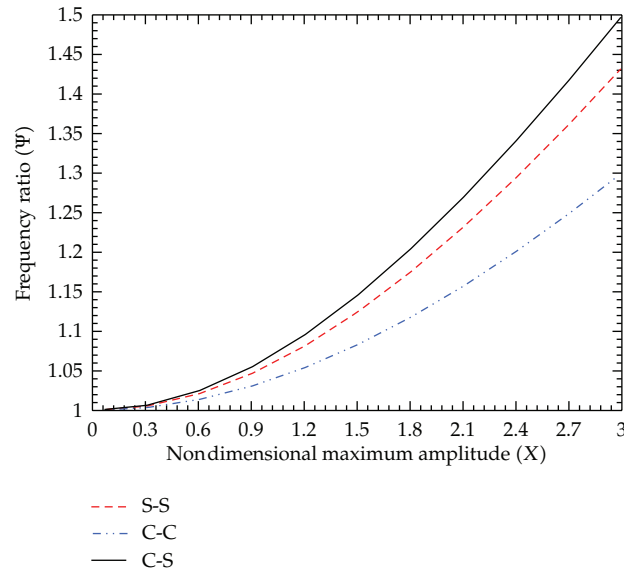


Figure 4: Nondimensional frequency ratio against nondimensional maximum amplitude of DWNTs under various boundary conditions ($k = 10^7$ N/m²).

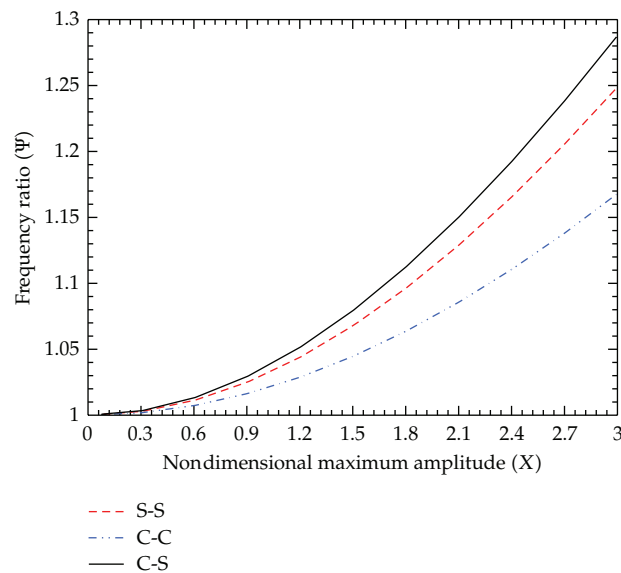


Figure 5: Nondimensional frequency ratio against nondimensional maximum amplitude of TWNTs under various boundary conditions ($k = 10^7$ N/m²).

results, the authors also calculate the variation of nondimensional amplitude ratio versus the linear period of vibration for the CNT center using fourth-order Runge-Kutta method. As can be seen in the figure, the results obtained using the HPM have a good agreement with numerical results. Using (3.21) and Table 1, the amplitude-space-time diagram of an SWNT

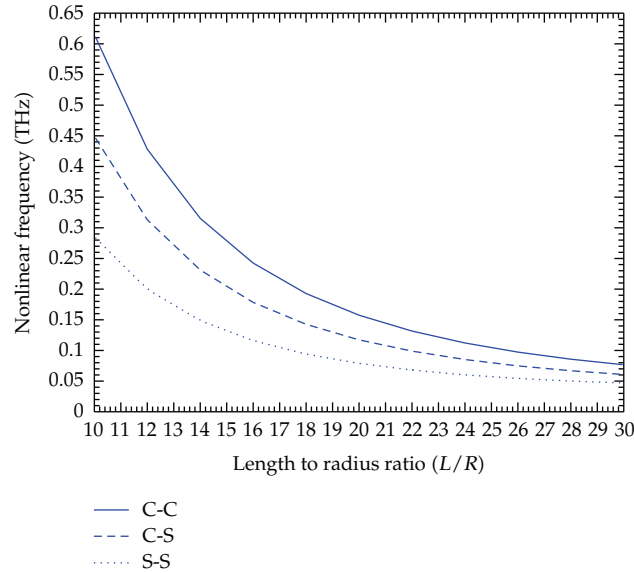


Figure 6: Fundamental nonlinear frequency against length to the outermost diameter ratio of a TWNT under different boundary conditions ($k = 10^7 \text{ N/m}^2$ and $X = 2$).

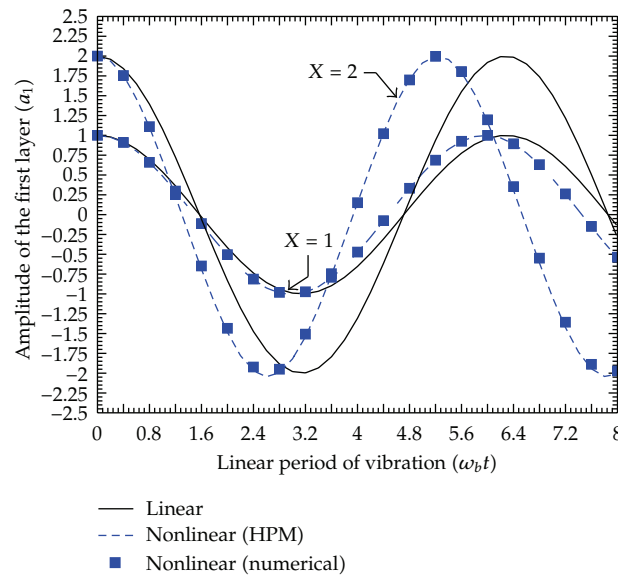


Figure 7: Variation of the nondimensional amplitude ratio versus the linear period of a C-C SWNT ($k = 10^7 \text{ N/m}^2$).

is plotted for S-S and C-C end conditions in Figures 8 and 9. The parameters used in these figures are $k = 10^7 \text{ N/m}^2$ and $X = 2$.

5. Conclusions

The HPM has been successfully used to investigate the nonlinear vibration analysis of multiwalled carbon nanotubes with arbitrary end conditions. The generated results obtained

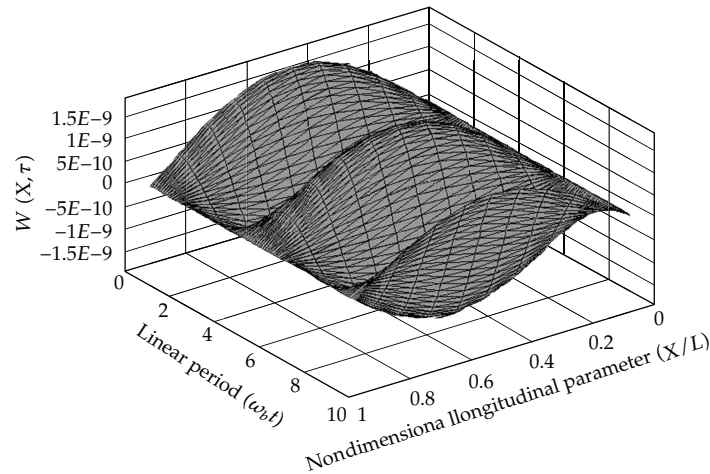


Figure 8: Amplitude-time-space diagram of an S-S SWNT ($k = 10^7$ N/m² and $X = 2$).

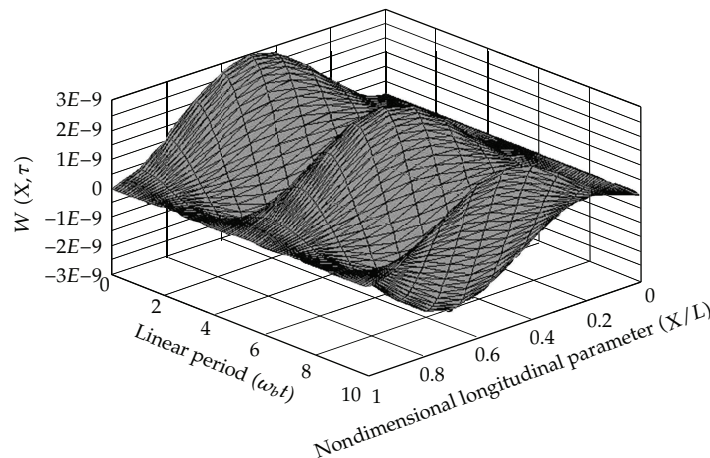


Figure 9: Amplitude-time-space diagram of a C-C SWNT ($k = 10^7$ N/m² and $X = 2$).

have been compared with those available in open literature, and excellent correlation has been achieved. The significant dependency of this oscillation to the surrounding elastic medium is observed. The nonlinear vibration frequency of nanotubes rises rapidly with increasing the amplitude especially when the stiffness of the medium is relatively small. For larger values of the medium stiffnesses (say $k > 10^8$ N/m²), the nonlinear vibration tends to the linear regime. It has been shown that with the increase of the aspect ratio of the nanotubes, the nonlinear vibration frequencies of MWNTs decrease. Also, as one travels through the end conditions of S-S, to fully clamped, denoted by C-C, respectively, the influence of the boundary conditions is shown to increase the natural frequencies. This effect is more significant for lower values of length to outermost diameter ratios. However, for higher values, the effect of the changes in the boundary conditions diminishes so that the corresponding natural frequencies are found to coincide.

The proposed method can be readily extended to the multiwalled CNTs with the number of walls more than three. It is worthwhile to mention that HPM is straightforward and powerful, and it is a promising technique for solving strong nonlinear partial differential equations.

References

- [1] S. Iijima, "Helical microtubules of graphitic carbon," *Nature*, vol. 354, no. 6348, pp. 56–58, 1991.
- [2] C. Q. Ru and K. M. Liew, "Elastic models for carbon nanotubes," in *Encyclopedia of Nanoscience and Nanotechnology*, vol. 4, pp. 1–14, 2003.
- [3] S. Adali, "Variational principles for multi-walled carbon nanotubes undergoing buckling based on nonlocal elasticity theory," *Physics Letters, Section A*, vol. 372, no. 35, pp. 5701–5705, 2008.
- [4] J. N. Ding, B. Kan, G. G. Cheng, Z. Fan, N. Y. Yuan, and Z. Y. Ling, "Numerical approach to torsion deformation of armchair single walled carbon nanotubes," *International Journal of Nonlinear Sciences and Numerical Simulation*, vol. 9, no. 4, pp. 309–314, 2008.
- [5] J. H. He, "An elementary introduction to recently developed asymptotic methods and nanomechanics in textile engineering," *International Journal of Modern Physics B*, vol. 22, no. 21, pp. 3487–3578, 2008.
- [6] I. Elishakoff and D. Pentaras, "Fundamental natural frequencies of double-walled carbon nanotubes," *Journal of Sound and Vibration*, vol. 322, no. 4–5, pp. 652–664, 2009.
- [7] C. Q. Ru, "Intrinsic vibration of multiwalled carbon nanotubes," *International Journal of Nonlinear Sciences and Numerical Simulation*, vol. 3, no. 3–4, p. 735, 2002.
- [8] S. B. Ye, R. P. S. Han, and L. H. Wang, "Oscillatory response of a capped double-walled carbon nanotube," *International Journal of Nonlinear Sciences and Numerical Simulation*, vol. 9, no. 4, pp. 339–346, 2008.
- [9] J. Yoon, C. Q. Ru, and A. Mioduchowski, "Noncoaxial resonance of an isolated multiwall carbon nanotube," *Physical Review B*, vol. 66, no. 23, Article ID 233402, pp. 2334021–2334024, 2002.
- [10] J. Yoon, C. Q. Ru, and A. Mioduchowski, "Vibration of an embedded multiwall carbon nanotube," *Composites Science and Technology*, vol. 63, no. 11, pp. 1533–1542, 2003.
- [11] Y. Zhang, G. Liu, and X. Han, "Transverse vibrations of double-walled carbon nanotubes under compressive axial load," *Physics Letters, Section A*, vol. 340, no. 1–4, pp. 258–266, 2005.
- [12] Y. M. Fu, J. W. Hong, and X. Q. Wang, "Analysis of nonlinear vibration for embedded carbon nanotubes," *Journal of Sound and Vibration*, vol. 296, no. 4–5, pp. 746–756, 2006.
- [13] J. H. He, "The homotopy perturbation method for nonlinear oscillators with discontinuities," *Applied Mathematics and Computation*, vol. 151, no. 1, pp. 287–292, 2004.
- [14] J. H. He, "Application of homotopy perturbation method to nonlinear wave equations," *Chaos, Solitons & Fractals*, vol. 26, no. 3, pp. 695–700, 2005.
- [15] J. H. He, "Homotopy perturbation method for solving boundary value problems," *Physics Letters, Section A*, vol. 350, no. 1–2, pp. 87–88, 2006.
- [16] J. H. He, "Limit cycle and bifurcation of nonlinear problems," *Chaos, Solitons & Fractals*, vol. 26, no. 3, pp. 827–833, 2005.
- [17] J. H. He, "Homotopy perturbation technique," *Computer Methods in Applied Mechanics and Engineering*, vol. 178, no. 3–4, pp. 257–262, 1999.
- [18] J. H. He, "Coupling method of a homotopy technique and a perturbation technique for non-linear problems," *International Journal of Non-Linear Mechanics*, vol. 35, no. 1, pp. 37–43, 2000.
- [19] J. H. He, "Comparison of homotopy perturbation method and homotopy analysis method," *Applied Mathematics and Computation*, vol. 156, no. 2, pp. 527–539, 2004.
- [20] J. H. He, "Homotopy perturbation method: a new nonlinear analytical technique," *Applied Mathematics and Computation*, vol. 135, no. 1, pp. 73–79, 2003.
- [21] J. H. He, "Some asymptotic methods for strongly nonlinear equations," *International Journal of Modern Physics B*, vol. 20, no. 10, pp. 1141–1199, 2006.
- [22] D. D. Ganji, "The application of He's homotopy perturbation method to nonlinear equations arising in heat transfer," *Physics Letters, Section A*, vol. 355, no. 4–5, pp. 337–341, 2006.
- [23] D. D. Ganji and A. Sadighi, "Application of homotopy-perturbation and variational iteration methods to nonlinear heat transfer and porous media equations," *Journal of Computational and Applied Mathematics*, vol. 207, no. 1, pp. 24–34, 2007.

- [24] A. Rajabi, D. D. Ganji, and H. Taherian, "Application of homotopy perturbation method in nonlinear heat conduction and convection equations," *Physics Letters, Section A*, vol. 360, no. 4-5, pp. 570–573, 2007.
- [25] S. Abbasbandy, "A numerical solution of Blasius equation by Adomian's decomposition method and comparison with homotopy perturbation method," *Chaos, Solitons & Fractals*, vol. 31, no. 1, pp. 257–260, 2007.
- [26] J. Biazar and H. Ghazvini, "Exact solutions for non-linear Schrödinger equations by He's homotopy perturbation method," *Physics Letters, Section A*, vol. 366, no. 1-2, pp. 79–84, 2007.
- [27] L. Cveticanin, "Application of homotopy-perturbation to non-linear partial differential equations," *Chaos, Solitons & Fractals*, vol. 40, no. 1, pp. 221–228, 2009.
- [28] A. Y. T. Leung and Z. Guo, "Homotopy perturbation for conservative Helmholtz-Duffing oscillators," *Journal of Sound and Vibration*, vol. 325, no. 1-2, pp. 287–296, 2009.
- [29] S. Abbasbandy, "Numerical solutions of the integral equations: homotopy perturbation method and Adomian's decomposition method," *Applied Mathematics and Computation*, vol. 173, no. 1, pp. 493–500, 2006.
- [30] J.-H. He, "Recent development of the homotopy perturbation method," *Topological Methods in Nonlinear Analysis*, vol. 31, no. 2, pp. 205–209, 2008.
- [31] J. Biazar and H. Aminikhah, "Study of convergence of homotopy perturbation method for systems of partial differential equations," *Computers and Mathematics with Applications*, vol. 58, no. 11-12, pp. 2221–2230, 2009.
- [32] H. T. Hahn and J. G. Williams, "Compression failure mechanisms in unidirectional composites," *Composite Materials*, vol. 7, pp. 115–139, 1984.
- [33] Y. Lanir and Y. C. B. Fung, "Fiber composite columns under compression," *Journal of Composite Materials*, vol. 6, pp. 387–402, 1972.
- [34] F.S. Tse, I. E. Morse, and R. T. Hinkle, *Mechanical Vibrations: Theory and Applications*, Allyn and Bacon Inc., Boston, Mass, USA, 2nd edition, 1978.
- [35] R. Ansari, M. Hemmatnezhad, and H. Ramezannezhad, "Application of HPM to the nonlinear vibrations of multiwalled carbon nanotubes," *Numerical Methods for Partial Differential Equations*, vol. 26, pp. 490–500, 2010.